Hindawi
Advances in Mathematical Physics
Volume 2017, Article ID 2837603, 9 pages
https://doi.org/10.1155/2017/2837603

Research Article

Nonlinear Hydroelastic Waves Generated due to a Floating Elastic Plate in a Current

Ping Wang,[1] Yongyan Wang,[2] Chuanqi Su,[2] and Yanzhao Yang[1]

[1]*School of Mathematics and Physics, Qingdao University of Science and Technology, Songling Road, Qingdao 266061, China*
[2]*College of Electromechanical Engineering, Qingdao University of Science and Technology, Songling Road, Qingdao 266061, China*

Correspondence should be addressed to Yongyan Wang; wangyongyan168@163.com

Received 25 March 2017; Accepted 10 July 2017; Published 13 December 2017

Academic Editor: Ming Mei

Effects of underlying uniform current on the nonlinear hydroelastic waves generated due to an infinite floating plate are studied analytically, under the hypotheses that the fluid is homogeneous, incompressible, and inviscid. For the case of irrotational motion, the Laplace equation is the governing equation, with the boundary conditions expressing a balance among the hydrodynamics, the uniform current, and elastic force. It is found that the convergent series solutions, obtained by the homotopy analysis method (HAM), consist of the nonlinear hydroelastic wave profile and the velocity potential. The impacts of important physical parameters are discussed in detail. With the increment of the following current intensity, we find that the amplitudes of the hydroelastic waves decrease very slightly, while the opposing current produces the opposite effect on the hydroelastic waves. Furthermore, the amplitudes of waves increase very obviously for higher opposing current speed but reduce very slightly for higher following current speed. A larger amplitude of the incident wave increases the hydroelastic wave deflections for both opposing and following current, while for Young's modulus of the plate there is the opposite effect.

1. Introduction

A floating elastic plate may be an appropriate physical model for a very large floating structure (VLFS) in the ocean or an ice sheet in the polar region due to its huge horizontal dimension compared with its vertical thickness. The nonlinear hydroelastic responses, without assuming that the waves are necessarily of small amplitude, become an indispensable factor during designing a VLFS or considering an ice sheet as a storage facility, a mobile offshore base or an aircraft runway, and so on. Forbes (1986) [1] studied preliminarily the nonlinear periodic waves beneath an elastic ice sheet in infinite water depths by the perturbation technology. Forbes (1988) [2] further optimized their previous method in the frame of perturbation technology by introducing Newton-Raphson techniques to approximate the Fourier coefficients. Vanden-Broeck and Părău (2011) [3] tried to extend the study of Forbes (1988) [2] to the large-amplitude periodic waves, while pointing out objectively that the perturbation method is not applicable to very steep waves for which it depended strongly on small parameters. The analytic solutions for the hydroelastic solitary waves propagating under an infinite elastic plate were derived by Milewski et al. (2011) [4], who used the asymptotic and numerical methods. Wang and Lu (2013) [5] investigated the nonlinear hydroelastic progressive waves traveling in an infinite elastic plate in deep water by the homotopy analysis method (HAM), which is completely independent of any small physical parameter [6]. Using the HAM in a similar way, the two-layer fluid was considered by Wang and Lu (2016) [7] to study the effects of the stratification of the fluid on the nonlinear hydroelastic waves traveling in an infinite elastic plate. It is found that a larger density ratio or depth ratio of the fluid layers can reduce the elastic plate deflection.

All the investigations mentioned above were under the hypothesis that there is no current in the oceanic environments. As we know, there are various reasons such as wind, thermal, earth's rotation, and tidal effects that frequently generate ocean currents. Some scholars analytically investigated nonlinear hydroelastic waves with a current. Employing the linear potential-flow theory, Schulkes et al. (1987) [8] first considered the effect of uniform flow beneath a floating ice

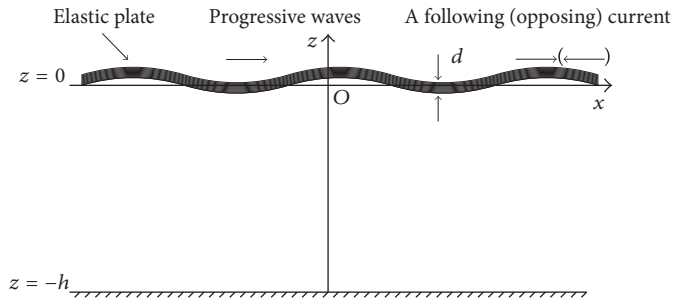

Figure 1: Coordinates.

plate. Bhattacharjee and Sahoo (2007) [9] used dispersion relation to analyze detailed characteristics of the flexural gravity waves due to a floating elastic plate in the presence of a following current or an opposing current. Asymptotic depressions for the transient flexural gravity resulting from initial disturbances at a point were derived subsequently by Bhattacharjee and Sahoo (2008) [10]. Mohanty et al. (2014) [11] studied a combined effect of current and compressive force on time-dependent flexural gravity wave motion in both the cases of single and two-layer fluids and obtained the asymptotic results for Green's function and the deflection of ice sheet using the method of stationary phase. Recently, Lu and Yeung (2015) [12] considered unsteady hydroelastic waves caused by the interaction of fixed concentrated line loads and the underlying current and found the flexural gravity wave motion depended on the ratio of current speed to phase or group speeds.

In this paper, we consider nonlinear hydroelastic waves generated due to a floating elastic plate in an underlying uniform current for the two-dimensional case. Two underlying currents are studied with the aid of the HAM. One is following current and the other is opposing current. Convergent analytical series solutions are deduced for the nonlinear hydroelastic response.

2. Mathematical Description

As shown in Figure 1, Cartesian coordinates oxz fixed on the earth are used, in which the x-axis coincides with the undisturbed plate-water interface, while the z-axis points vertically upward. The floating plate extends to the infinity along the x-axis without draft, and an underlying following current is assumed to be moving from the left to right (an opposing current is from the right to left). Under the assumptions that the fluid is homogeneous, incompressible, and inviscid and the flow is irrotational, the governing equation is

$$\nabla^2\phi = 0, \quad (z \le \zeta(x,t)), \tag{1}$$

where $\phi(x,z,t)$ is the wave velocity potential. $z = \zeta(x,t)$ is the hydroelastic wave elevation of the wave-plate interface and also is the vertical hydroelastic response of the floating plate. t is the time from the start.

The bottom condition at deep water reads

$$\frac{\partial\phi}{\partial z} = 0, \quad (z = -\infty). \tag{2}$$

The flexural rigidity of the plate is denoted by $D = Ed^3/[12(1-\nu^2)]$, where E, d, and ν are Young's modulus, the constant thickness, and Poisson's ratio of the plate, respectively. Let U be the intensity of the uniform current, and let $m_e = \rho_e d$ be the mass of the plate in a unit length, where p_e is the uniform densities of elastic plate. ρ is the uniform densities of the fluid. The nonlinear kinematic and dynamic boundary conditions on the unknown plate-water interface $z = \zeta(x,t)$ are given by

$$\begin{aligned}
&\frac{\partial\zeta}{\partial t} + \frac{\partial\phi}{\partial x}\frac{\partial\zeta}{\partial x} + U\frac{\partial\zeta}{\partial x} - \frac{\partial\phi}{\partial z} = 0,\\
&\rho\left[\frac{\partial\phi}{\partial t} + \frac{1}{2}\left(|\nabla\phi|^2 + U^2\right) + U\frac{\partial\phi}{\partial x} + g\zeta\right] + D\nabla^4\zeta\\
&\quad + m_e\left(\frac{\partial^2\zeta}{\partial t^2} + g\right) = 0.
\end{aligned} \tag{3}$$

As for the progressive waves, we introduced an independent variable as follows:

$$X = kx - \omega t, \tag{4}$$

where k and ω are the wave number and the angular frequency of the incident wave, respectively. So we can perform the velocity potential function $\phi(x,z,t) = \phi(X,z)$ and the hydroelastic wave profile $\zeta(x,t) = \zeta(X)$.

To simplify the formulation, the physical variables are nondimensionalized as

$$U^* = U\left(\frac{k}{g}\right)^{1/2},$$

$$x^* = kx,$$

$$z^* = kz,$$

$$
\begin{aligned}
t^* &= t\left(gk\right)^{1/2},\\
d^* &= kd,\\
\phi^* &= \frac{k^2\phi}{\left(gk\right)^{1/2}},\\
\zeta^* &= k\zeta,\\
\omega^* &= \frac{\omega}{\left(gk\right)^{1/2}},\\
D^* &= \frac{k^4 D}{\left(\rho g\right)},\\
\rho_e^* &= \frac{\rho_e}{\rho},\\
m_e^* &= \frac{km_e}{\rho},\\
E^* &= \frac{kE}{\left(\rho g\right)}.
\end{aligned}
\tag{5}
$$

By transformation (4) and nondimensionalization (5), (1)–(3) are changed into (after omitting the $*$)

$$
\frac{\partial^2\phi}{\partial X^2} + \frac{\partial^2\phi}{\partial z^2} = 0, \quad \left(z \le \zeta\left(X\right)\right), \tag{6}
$$

$$
\frac{\partial\phi}{\partial z} = 0, \quad \left(z = -\infty\right), \tag{7}
$$

$$
-\omega\frac{\mathrm{d}\zeta}{\mathrm{d}X} + \frac{\partial\phi}{\partial X}\frac{\mathrm{d}\zeta}{\mathrm{d}X} + U\frac{\mathrm{d}\zeta}{\mathrm{d}X} - \frac{\partial\phi}{\partial z} = 0, \quad \left(z = \zeta\left(X\right)\right), \tag{8}
$$

$$
\begin{aligned}
&-\left(\omega - U\right)\frac{\partial\phi}{\partial X} + f + \frac{1}{2}U^2 + \zeta + D\frac{\mathrm{d}^4\zeta}{\mathrm{d}X^4}\\
&\quad + m_e\left(\omega^2\frac{\mathrm{d}^2\zeta}{\mathrm{d}X^2} + 1\right) = 0, \quad \left(z = \zeta\left(X\right)\right),
\end{aligned}
\tag{9}
$$

respectively, where

$$
f = \frac{1}{2}\left[\left(\frac{\partial\phi}{\partial X}\right)^2 + \left(\frac{\partial\phi}{\partial z}\right)^2\right]. \tag{10}
$$

A partial combination of (8) and (9) gives the boundary conditions on $z = \zeta(X)$ as follows:

$$
\begin{aligned}
&\omega\left(\omega - U\right)\frac{\partial^2\phi}{\partial X^2} + \frac{\partial\phi}{\partial z} - \omega\frac{\partial f}{\partial X} - \omega D\frac{\mathrm{d}^5\zeta}{\mathrm{d}X^5} - \omega^3 m_e\frac{\mathrm{d}^3\zeta}{\mathrm{d}X^3}\\
&\quad - \left(\frac{\partial\phi}{\partial X} + U\right)\frac{\mathrm{d}\zeta}{\mathrm{d}X} = 0.
\end{aligned}
\tag{11}
$$

For a given angular frequency ω or the current speed U, the unknown velocity potential $\phi(X, z)$ and the hydroelastic waves $\zeta(X)$ are obtained from (6), (7), (9), and (11) by using the HAM in the subsequent sections.

3. Analytical Approach Based on the HAM

3.1. Solution Expressions. We first predict a set of solution expressions of the unknown nonlinear hydroelastic waves. From physical points of view, unknown velocity potential and progressive hydroelastic wave deflections generated due to a thin elastic plate can be expressed by [5]

$$
\begin{aligned}
\phi\left(X, z\right) &= \sum_{i=0}^{+\infty}\alpha_i \exp\left(iz\right)\sin\left(iX\right),\\
\zeta\left(X\right) &= \sum_{i=0}^{+\infty}\beta_i \cos\left(iX\right),
\end{aligned}
\tag{12}
$$

with the base functions $\exp(iz)\sin(iX)$ $(i \ge 0)$ and $\cos(iX)$ $(i \ge 0)$, respectively, where β_i and α_i are all unknown coefficients to be derived.

According to the solution expressions (12), we can construct the initial estimation of the potential function as

$$
\phi_0\left(X, z\right) = \alpha_{0,1}\exp\left(z\right)\sin\left(X\right), \tag{13}
$$

where $\alpha_{0,1}$ is an unknown coefficient. We choose

$$
\zeta_0\left(X\right) = 0 \tag{14}
$$

as the initial estimation of the hydroelastic wave deflection to simplify the computation [5, 6]. Considering the nondimensionalized linear dispersion relation [9] for deep water with a current, we think that the initial estimation of the nonlinear dispersion relation satisfies

$$
\left(\omega_0 - U_0\right)^2 = D - m_e + 1, \tag{15}
$$

where ω_0 is the initial estimation of angular frequency ω and U_0 is the initial estimation of the uniform current intensity U.

3.2. Zeroth-Order Deformation Equations. Instead of solving these nonlinear equations (6), (7), (9), and (11) directly, we develop four topology homotopies $\Phi(X, z; q)$, $\eta(X; q)$, $\omega(q)$, and $U(q)$. As the embedding parameter $q \in [0, 1]$ increases from 0 to 1 and $\Phi(X, z; q)$ deforms continuously from its initial estimation $\phi_0(X, z)$ to the exact solution $\phi(X, z)$, $\eta(X; q)$ varies continuously from $\zeta_0(X)$ to $\zeta(X)$, $\omega(q)$ is from ω_0 to ω, and $U(q)$ is from U_0 to U. The homotopies $\Phi(X, z; q)$ and $\eta(X; q)$ are governed by the zeroth-order deformation equations for (6), (7), (9), and (11) as follows:

$$
\frac{\partial^2\Phi\left(X, z; q\right)}{\partial X^2} + \frac{\partial^2\Phi\left(X, z; q\right)}{\partial z^2} = 0, \quad \left(z \le \eta\left(X; q\right)\right), \tag{16}
$$

$$
\frac{\partial\Phi\left(X, z; q\right)}{\partial z} = 0, \quad \left(z = -\infty\right), \tag{17}
$$

$$
\begin{aligned}
&\left(1 - q\right)\mathscr{L}_1\left[\Phi\left(X, z; q\right) - \phi_0\left(X, z\right)\right]\\
&\quad = qc_0\mathscr{N}_1\left[\Phi\left(X, z; q\right), \eta\left(X; q\right)\right], \quad \left(z = \eta\left(X; q\right)\right),
\end{aligned}
\tag{18}
$$

$$
\begin{aligned}
&\left(1 - q\right)\mathscr{L}_2\left[\eta\left(X; q\right) - \zeta_0\left(X\right)\right]\\
&\quad = qc_0\mathscr{N}_2\left[\eta\left(X; q\right), \Phi\left(X, z; q\right)\right], \quad \left(z = \eta\left(X; q\right)\right),
\end{aligned}
\tag{19}
$$

where c_0 is a nonzero convergence-control parameter. Based on the nonlinear boundary conditions (11) and (9), respectively, $\mathcal{N}_1[\cdot]$ and $\mathcal{N}_2[\cdot]$ are the nonlinear operators defined by

$$\begin{aligned}
&\mathcal{N}_1\left[\Phi\left(X,z;q\right),\eta\left(X;q\right)\right]\\
&\quad=\omega\left(\omega-U\right)\frac{\partial^2\Phi}{\partial X^2}+\frac{\partial\Phi}{\partial z}-\omega\frac{\partial F}{\partial X}-\omega D\frac{\partial^5\eta}{\partial X^5}\\
&\qquad-\omega^3 m_e\frac{\partial^3\eta}{\partial X^3}-\left(\frac{\partial\Phi}{\partial X}+U\right)\frac{\partial\eta}{\partial X},\\
&\mathcal{N}_2\left[\eta\left(X;q\right),\Phi\left(X,z;q\right)\right]\\
&\quad=-\left(\omega-U\right)\frac{\partial\Phi}{\partial X}+F+\frac{1}{2}U^2+\eta+D\frac{\partial^4\eta}{\partial X^4}\\
&\qquad+m_e\left(\omega^2\frac{\partial^2\eta}{\partial X^2}+1\right),
\end{aligned}\tag{20}$$

respectively, where

$$F=\frac{1}{2}\left[\left(\frac{\partial\Phi}{\partial X}\right)^2+\left(\frac{\partial\Phi}{\partial z}\right)^2\right].\tag{21}$$

We choose the linear operators of the wave profile function $\eta(X;q)$ in the nonlinear operator $\mathcal{N}_2$ as the auxiliary linear operator $\mathcal{L}_2$:

$$\mathcal{L}_2\left[\eta\left(X;q\right)\right]=\frac{\partial^4\eta}{\partial X^4}+\frac{\partial^2\eta}{\partial X^2}+\eta,\tag{22}$$

where $\mathcal{L}_2[0]=0$.

Expanding these unknown variables $\Phi(X,z;q)$, $\eta(X;q)$, $\omega(q)$, and $U(q)$ into the Taylor series about q at $q=0$:

$$\begin{aligned}
\Phi\left(X,z;q\right)&=\sum_{m=0}^{+\infty}\phi_m\left(X,z\right)q^m,\\
\eta\left(X;q\right)&=\sum_{m=0}^{+\infty}\zeta_m\left(X\right)q^m,\\
\omega\left(q\right)&=\sum_{m=0}^{+\infty}\omega_m q^m,\\
U\left(q\right)&=\sum_{m=0}^{+\infty}U_m q^m,
\end{aligned}\tag{23}$$

where

$$\begin{aligned}
&\left\{\phi_m\left(X,z\right),\zeta_m\left(X\right),\omega_m,U_m\right\}\\
&\quad=\frac{1}{m!}\frac{\partial^m}{\partial q^m}\left\{\Phi\left(X,z;q\right),\eta\left(X;q\right),\omega\left(q\right),U\left(q\right)\right\}\Big|_{q=0}.
\end{aligned}\tag{24}$$

We choose the linear operators of $\Phi(X,z;q)$ in $\mathcal{N}_1$ as the auxiliary linear operator $\mathcal{L}_1$:

$$\mathcal{L}_1\left[\Phi\left(X,z;q\right)\right]=\omega_0\left(\omega_0-U_0\right)\frac{\partial^2\Phi}{\partial X^2}+\frac{\partial\Phi}{\partial z},\tag{25}$$

where $\mathcal{L}_1[0]=0$. In particular, we have great freedom to choose the auxiliary linear operator in the HAM, and based on the linear wave theory, the angular frequency and the current speed can be approximated as $\omega\approx\omega_0$ and $U\approx U_0$ in the operator $\mathcal{L}_1$, respectively.

Once c_0 is so properly chosen that the series in (23) converge at $q=1$, we would obtain their convergent homotopy-series solutions.

3.3. High-Order Deformation Equations. Differentiating the zero-order deformation equations (16)–(19) m times about q, then dividing them by $m!$, and setting $q=0$, we obtain the linear PDES for the unknown variables $\phi_m(X,z)$, $\zeta_m(X)$, ω_m, and U_m, namely, the mth-order deformation equations:

$$\begin{aligned}
\frac{\partial^2\phi_m\left(X,z\right)}{\partial X^2}+\frac{\partial^2\phi_m\left(X,z\right)}{\partial z^2}&=0,\quad\left(z\le 0\right),\\
\frac{\partial\phi_m\left(X,z\right)}{\partial z}&=0,\quad\left(z=-\infty\right),
\end{aligned}\tag{26}$$

where $m\ge 1$.

$$\mathcal{L}_1\left(\phi_m\right)\big|_{z=0}=c_0\Delta^{\phi}_{m-1}+H_m S_{m-1}-\overline{S}_m,\quad\left(z=0\right)\tag{27}$$

$$\begin{aligned}
\mathcal{L}_2\left(\zeta_m\right)&=c_0\Delta^{\zeta}_{m-1}\\
&\quad+H_m\left(\frac{\mathrm{d}^4\zeta_{m-1}}{\mathrm{d}X^4}+\frac{\mathrm{d}^2\zeta_{m-1}}{\mathrm{d}X^2}+\zeta_{m-1}\right),\quad\left(z=0\right),
\end{aligned}\tag{28}$$

where $H_m=H(m-2)$ and $H(\cdot)$ is the Heviside step function. The elaborated expressions for Δ^{ϕ}_{m-1}, S_{m-1}, $\overline{S}_m$, and Δ^{ζ}_{m-1} are given in Appendix.

In the first-order calculation, we still can not get the coefficient $\alpha_{0,1}$, so an additional equation is introduced to relate the hydroelastic wave height and the incident wave height H as

$$\zeta_1\left(m\pi\right)-\zeta_1\left(n\pi\right)=H=2a,\tag{29}$$

where m is an even integer, n an odd integer, and a the dimensionless amplitude of first-order incident wave.

3.4. Optimal Convergence-Control Parameters. According to Liao [6, 13], it is the convergence-control parameter c_0 that essentially differs the HAM from all other analytic techniques. We can obtain the convergent approximate series solutions by choosing the optimal c_0. For given the number M of the discrete point, the optimal c_0 corresponds to the fastest decrease of the total squared residual ε^T_m defined by

$$\varepsilon^T_m=\varepsilon^{\phi}_m+\varepsilon^{\zeta}_m,\tag{30}$$

where

$$\begin{aligned}
\varepsilon^{\phi}_m&=\frac{1}{1+M}\sum_{i=0}^{M}\left(\mathcal{N}_1\left[\phi\left(X,z\right),\zeta\left(X\right)\right]\big|_{X=i\Delta X}\right)^2,\\
\varepsilon^{\zeta}_m&=\frac{1}{1+M}\sum_{i=0}^{M}\left(\mathcal{N}_2\left[\phi\left(X,z\right),\zeta\left(X\right)\right]\big|_{X=i\Delta X}\right)^2,
\end{aligned}\tag{31}$$

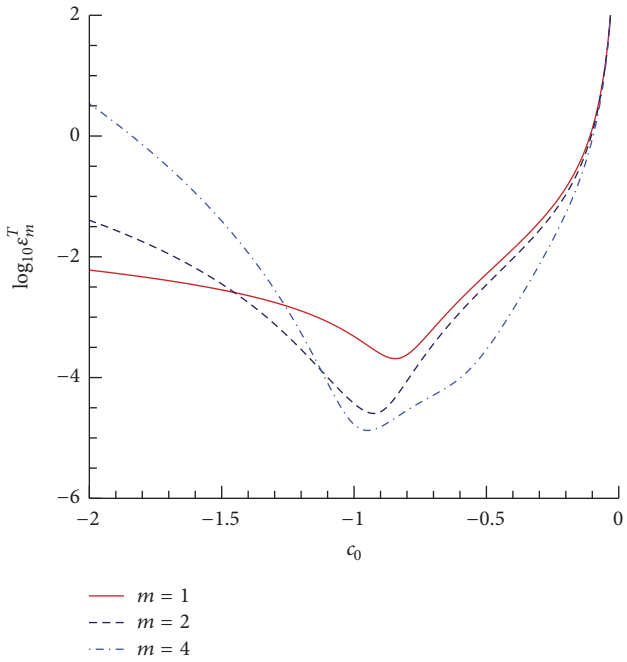

FIGURE 2: Residual squares of $\log_{10}\varepsilon_m^T$ of the mth-order homotopy approximation c_0. Solid line, $m = 1$; long dashed line, $m = 2$; dash-dotted line, $m = 4$.

where ε_m^ϕ and ε_m^ζ are the residual square errors of boundary conditions (18) and (19) at $q = 1$, respectively. $\Delta X = \pi/M$. We choose $M = 10$ here, and the optimal convergence-control parameter c_0 can be chosen by the minimum of ε_m^T in residual plot as shown in Figure 2.

4. Results and Discussion

The total residual square error ε_m^T at several different orders is illustrated for a fluid with the uniform current versus c_0 to show the validity and accuracy of our analytic solutions in Figure 2 with the case of $U_0 = 0.3$, $a = 0.1$, $\rho_e = 0.9$, $d = 0.005$, $E = 10^9$, and $\nu = 0.33$. It is found that, as the order m increases gradually, ε_m^T reduces to a minimum in the interval $-1.5 \le x \le -0.5$ and then the optimal c_0 is about -0.95. Further, we find from Table 1 that, as $c_0 = -0.95$, the square error ε_m^T decreases quickly to 7.26×10^{-7} at the 7th-order approximation.

We consider the effects of several important physical parameters, including the uniform current intensity and direction, the amplitude of incident wave, and Young's modulus of the floating plate, on the nonlinear dynamics characteristic of the hydroelastic waves. Firstly, Figure 3 shows variation of the hydroelastic wave deflection for different current intensity. As the maximum current speed U is about 1.5 m/s in ocean [14], we select four dimensionless current intensities 0 (without currents), 0.1, 0.2, and 0.3 in our computations. From the comparison between the following current and the opposing current, it is shown that the amplitudes of the hydroelastic waves decrease slightly with the increment of the following current intensity, while

TABLE 1: The total residual square error ε_m^T for different approximation order m with $c_0 = -0.95$.

m	ε_m^T
1	3.43×10^{-4}
2	2.68×10^{-5}
4	1.61×10^{-5}
7	7.26×10^{-7}

the opposing current has obvious opposite effects. Further, the hydroelastic wave is more greatly affected by the opposing current.

In Figures 4 and 5, three dimensionless amplitudes a are considered to examine the variation of the hydroelastic waves by increasing a from 0.01 to 0.1 for different current. We find that for both a following current and an opposing current a larger a increases the hydroelastic waves profile. In the following current case, we can observe from Figure 4 that a larger current intensity reduces the hydroelastic wave profile very slightly, while for the opposing current case, we note from Figure 5 that amplitude of the hydroelastic waves increases obviously with the increment of the current intensity U.

Finally, we consider the effects of Young's modulus E of the floating plate on the hydroelastic waves by increasing E from 10^9 to 10^{11} for different current. It is seen from Figures 6 and 7 that for both a following current and an opposing current a larger E decays the waves' amplitude. It is because the plate becomes stiffer so that a large reactive force can be generated to resist the deformation of the hydroelastic waves. Particularly in the following current case, Figure 6 indicates that for a larger U the wave amplitude reduces very slightly, while for the opposing current case, we observe from Figure 7 that amplitude of the hydroelastic wave increases very obviously with the increment of current intensity U.

5. Conclusions

We extend the study by Wang and Lu (2013) [5] to the nonlinear hydroelastic waves on an underlying uniform current, which describes wave-current interaction in the real ocean. In the frame of the HAM, we construct the zeroth-order deformation equations, in which we choose the auxiliary linear operator $\mathscr{L}_1$ containing only the derivatives of $\Phi(X, z; q)$ in nonlinear operator $\mathscr{N}_1$ and $\mathscr{L}_2$ containing only the derivatives of $\eta(X; q)$ in nonlinear operator $\mathscr{N}_2$. In particular, we choose the corresponding linear solutions as the initial estimations of the dispersion relation, the velocity potential $\phi(X, z)$, and the hydroelastic waves profile $\zeta(X)$, respectively. The convergent solutions are analytically achieved by solving the mth-order deformation equations, and numerical results indicate the convergence and accuracy of our HAM-based analytical expressions by choosing the optimal c_0.

The influences of important physical parameters on the nonlinear hydroelastic waves in the underlying uniform current are discussed in detail. It is found that in the

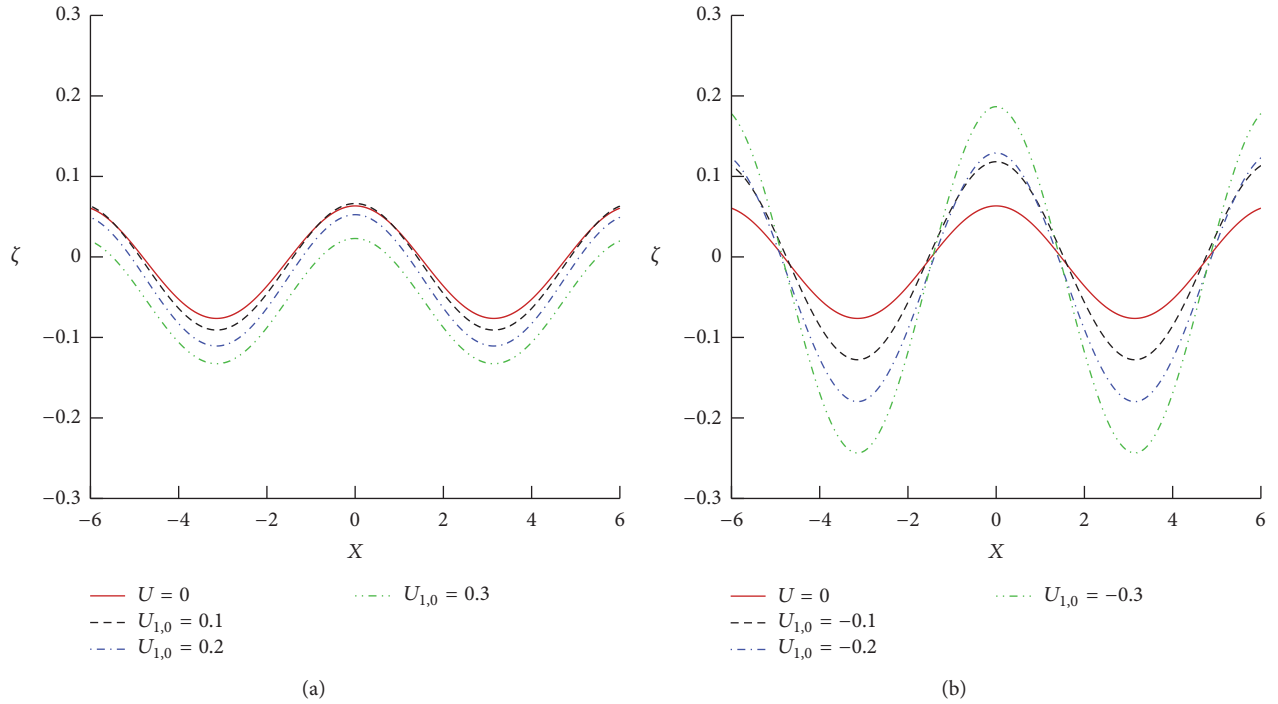

FIGURE 3: Variation of the hydroelastic wave profiles versus x for different current speed $U_{1,0}$. (a) A following current. (b) An opposing current.

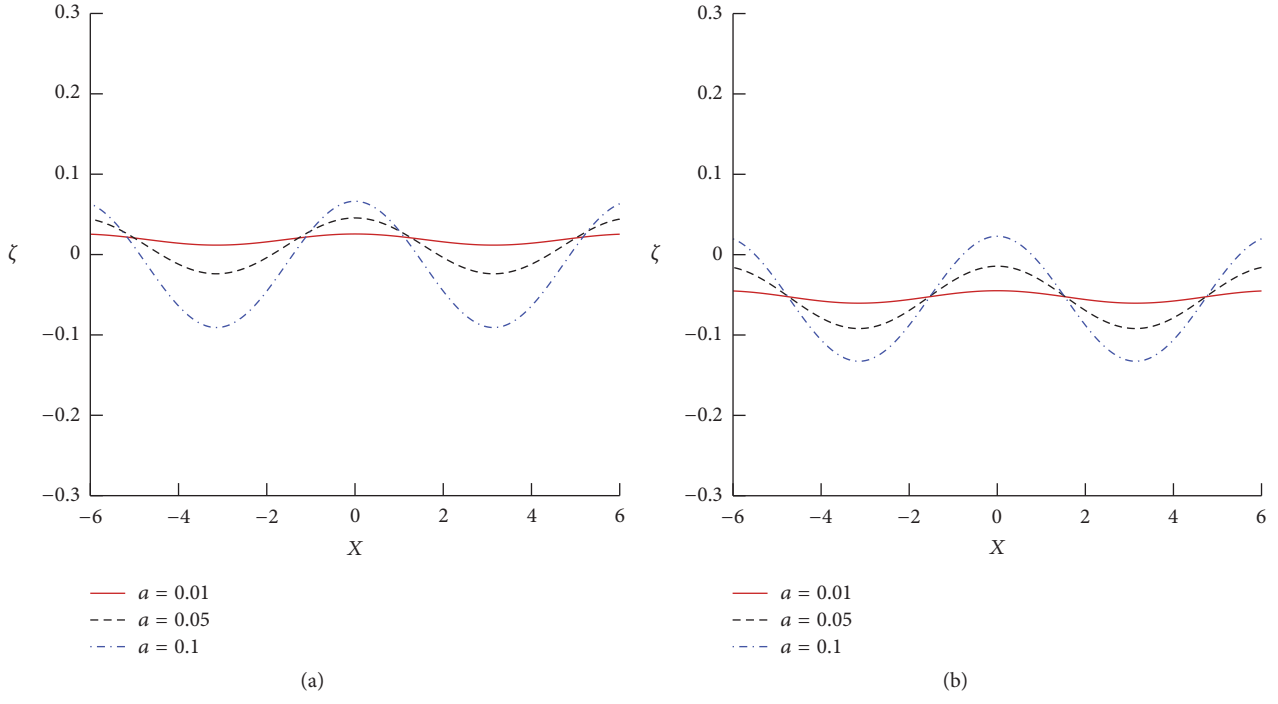

FIGURE 4: Variation of the plate hydroelastic deflection versus x for different wave amplitude a on a following current. (a) $U_{1,0} = 0.1$. (b) $U_{1,0} = 0.3$.

following current case a larger U reduces the amplitude of the hydroelastic waves very slightly but increases it obviously in an opposing current. The hydroelastic waves become steeper for both following and opposing current as the incident wave amplitudes a increase, but Young's modulus E has the opposite effect on the hydroelastic waves. Further, the hydroelastic wave is more greatly affected by the opposing current. Particularly, the hydroelastic wave is more greatly affected by the opposing current than by the following current.

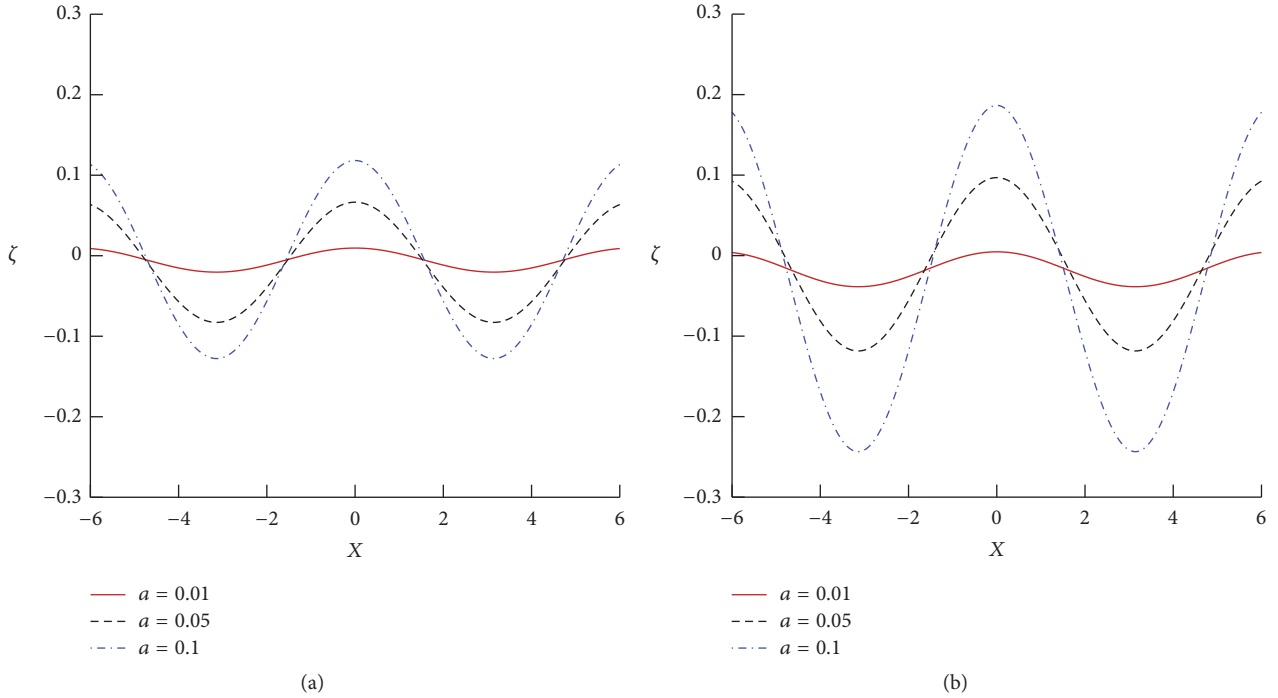

Figure 5: Variation of the hydroelastic wave profiles versus x for different wave amplitude a on an opposing current. (a) $U_{1,0} = -0.1$. (b) $U_{1,0} = -0.3$.

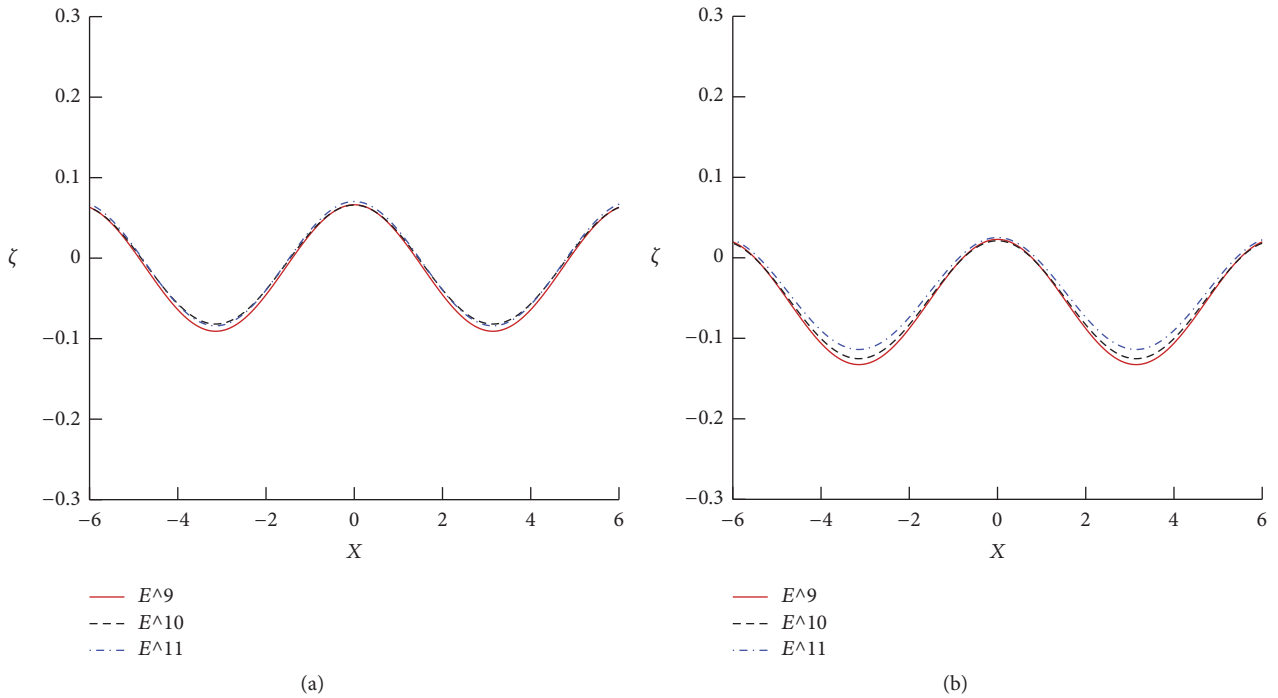

Figure 6: Variation of the hydroelastic wave profiles versus x for different value of Young's modulus on a following current. (a) $U_{1,0} = 0.1$. (b) $U_{1,0} = 0.3$.

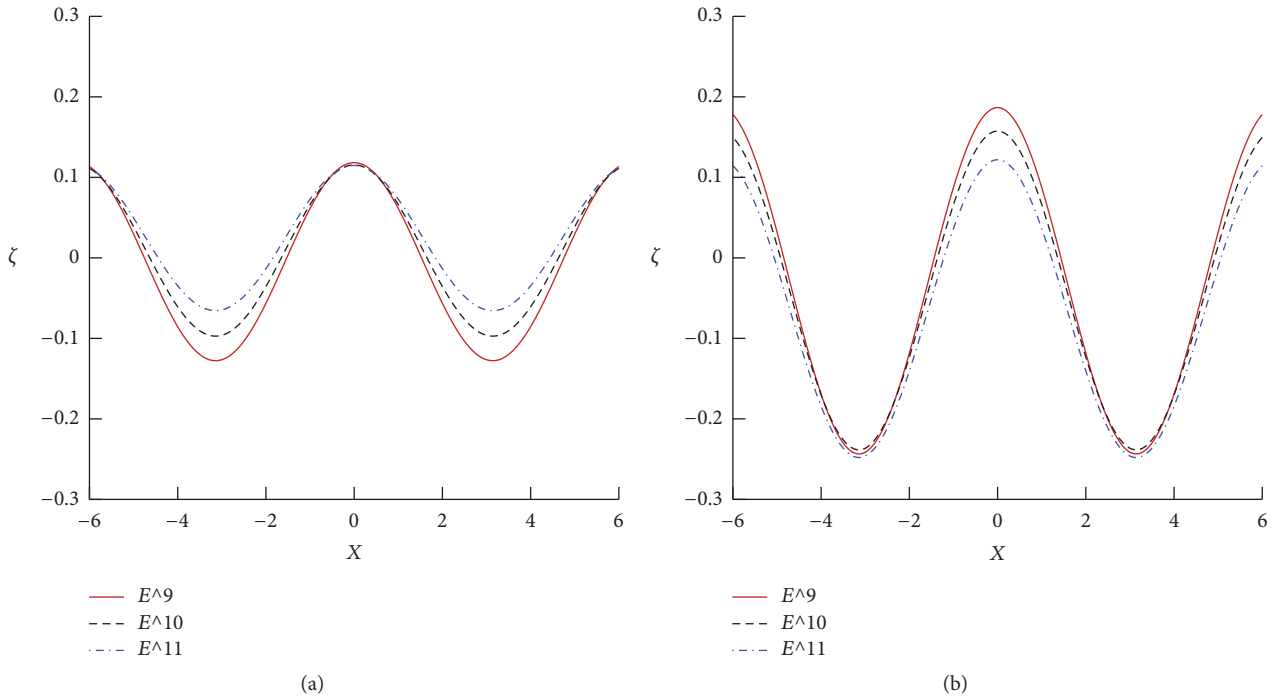

FIGURE 7: Variation of the hydroelastic wave profiles x for different value of Young's modulus on an opposing current. $U_{1,0} = -0.1$. (b) $U_{1,0} = -0.3$.

Appendix

Detailed Derivation of Δ^{ϕ}_{m-1}, S_{m-1}, $\overline{S}_m$, and Δ^{ζ}_{m-1} in (27) and (28)

Let

$$\eta^n = \left(\sum_{i=1}^{+\infty} \zeta_i q^i\right)^n = \sum_{i=n}^{+\infty} \mu_{n,i} q^i. \tag{A.1}$$

We have a Maclaurin series for any z as follows:

$$\phi_m(X, z) = \sum_{n=0}^{+\infty} \frac{1}{n!} \left.\frac{\partial^n \phi_m}{\partial z^n}\right|_{z=0} z^n. \tag{A.2}$$

For $z = \eta(X; q)$, it follows from (A.1) and (A.2) that

$$\begin{aligned}\phi_m(X, \eta) &= \sum_{n=0}^{+\infty} \left(\frac{1}{n!} \left.\frac{\partial^n \phi_m}{\partial z^n}\right|_{z=0}\right) \left(\sum_{i=n}^{+\infty} \mu_{n,i} q^i\right) \\ &= \sum_{i=0}^{+\infty} \psi_{m,i} q^i,\end{aligned} \tag{A.3}$$

where

$$\psi_{m,i} = \sum_{n=0}^{i} \left(\frac{1}{n!} \left.\frac{\partial^n \phi_m}{\partial z^n}\right|_{z=0}\right) \mu_{n,i}. \tag{A.4}$$

Thus, for $z = \eta(X; q)$, we have

$$\begin{aligned}\Phi(X, \eta; q) &= \sum_{m=0}^{+\infty} \phi_m(X, \eta) q^m = \sum_{m=0}^{+\infty} \left(\sum_{i=0}^{+\infty} \psi_{m,i} q^i\right) q^m \\ &= \sum_{m=0}^{+\infty} \varphi_m q^m,\end{aligned} \tag{A.5}$$

where

$$\varphi_m = \sum_{i=0}^{m} \psi_{m-i,i}. \tag{A.6}$$

Let

$$\omega^n = \left(\sum_{i=0}^{+\infty} \omega_i q^i\right)^n = \sum_{i=0}^{+\infty} \omega_{n,i} q^i. \tag{A.7}$$

Substituting series expansions (A.1), (A.5), and (A.7) into conditions (18) and (19) and then equating the like-power of q, we acquire two linear boundary conditions (27) and (28), respectively. Then the explicit expressions for Δ^{ϕ}_{m-1}, S_{m-1}, $\overline{S}_m$, and Δ^{ζ}_{m-1} in these two conditions are derived by

$$\begin{aligned}&\Delta^{\phi}_{m-1} \\ &= \sum_{j=0}^{m-1} \sum_{i=0}^{j} \omega_{m-1-j} \left(\omega_{j-i} - U_{j-i}\right) \frac{\mathrm{d}^2 \varphi_i}{\mathrm{d}X^2} + \overline{\varphi}_{m-1} \\ &\quad - D \sum_{i=0}^{m-1} \omega_{m-1-i} \frac{\mathrm{d}^5 \zeta_i}{\mathrm{d}X^5}\end{aligned}$$

$$
\begin{aligned}
&- \sum_{j=0}^{m-1}\sum_{i=0}^{j} \omega_{m-1-j}\left(\frac{\mathrm{d}\varphi_i}{\mathrm{d}X}\frac{\mathrm{d}^2\varphi_{j-i}}{\mathrm{d}X^2} + \overline{\varphi}_i\frac{\mathrm{d}\overline{\varphi}_{j-i}}{\mathrm{d}X}\right)\\
&- m_e\sum_{i=1}^{m-1} w_{3,m-1-i}\frac{\mathrm{d}^3\zeta_i}{\mathrm{d}X^3}\\
&- \sum_{i=0}^{m-1}\left(\frac{\mathrm{d}\varphi_i}{\mathrm{d}X} + U_i\right)\frac{\mathrm{d}\zeta_{m-1-i}}{\mathrm{d}X},
\end{aligned}
$$

$$
S_{m-1} = \sum_{i=0}^{m-2}\left[\omega_0\left(\omega_0 - U_0\right)\frac{\mathrm{d}^2\psi_{m-1-i,i}}{\mathrm{d}X^2} + \gamma_{m-1-i,i}\right],
$$

$$
\overline{S}_m = \sum_{i=1}^{m-1}\left[\omega_0\left(\omega_0 - U_0\right)\frac{\mathrm{d}^2\psi_{m-i,i}}{\mathrm{d}X^2} + \gamma_{m-i,i}\right],
$$

$$
\begin{aligned}
&\Delta_{m-1}^{\zeta}\\
&= -\sum_{i=0}^{m-1}\left(\omega_{m-1-i} - U_{m-1-i}\right)\frac{\mathrm{d}\varphi_i}{\mathrm{d}X}\\
&\quad + \frac{1}{2}\sum_{i=0}^{m-1}\left(\frac{\mathrm{d}\varphi_i}{\mathrm{d}X}\frac{\mathrm{d}\varphi_{m-1-i}}{\mathrm{d}X} + \overline{\varphi}_i\overline{\varphi}_{m-1-i} + U_iU_{m-1-i}\right)\\
&\quad + \zeta_{m-1} + D\frac{\mathrm{d}^4\zeta_{m-1}}{\mathrm{d}X^4} + m_e\sum_{i=0}^{m-1} w_{2,m-1-i}\frac{\mathrm{d}^2\zeta_i}{\mathrm{d}X^2},\\
&\qquad\qquad (m \geq 2),
\end{aligned}
$$

$$
\begin{aligned}
&\Delta_0^{\zeta}\\
&= \frac{1}{2}\left[\left(\frac{\mathrm{d}\varphi_0}{\mathrm{d}X}\right)^2 + \overline{\varphi}_0^2 + U_0^2\right] - \left(\omega_0 - U_0\right)\frac{\mathrm{d}\varphi_0}{\mathrm{d}X}\\
&\quad + m_e,
\end{aligned}
\tag{A.8}
$$

where

$$
\begin{aligned}
\overline{\varphi}_m &= \sum_{i=0}^{m}\gamma_{m-i,i},\\
\gamma_{m-i,i} &= \sum_{n=0}^{i}\frac{1}{n!}\left(\left.\frac{\partial^{n+1}\phi_{m-i}}{\partial z^{n+1}}\right|_{z=0}\right)\mu_{n,i}.
\end{aligned}
\tag{A.9}
$$

Disclosure

The authors themselves programed the symbolic computation software named Mathematica 8.0 independently to gain the approximate analytical solutions of the PDEs considered here.

Conflicts of Interest

There are no conflicts of interest regarding this manuscript.

Acknowledgments

This research was financially supported by the National Natural Science Foundation of China under Grant no. 51374134 and Project of Shandong Province Higher Educational Science and Technology Program no. J14LJ53. Qingdao Postdoctoral Applied Research Project no. 020022034 is also acknowledged.

References

[1] L. K. Forbes, "Surface waves of large amplitude beneath an elastic sheet. I. High-order series solution," *Journal of Fluid Mechanics*, vol. 169, pp. 409–428, 1986.

[2] L. K. Forbes, "Surface waves of large amplitude beneath an elastic sheet. part 2. Galerkin solution," *Journal of Fluid Mechanics*, vol. 188, pp. 491–508, 1988.

[3] J.-M. Vanden-Broeck and E. I. Părău, "Two-dimensional generalized solitary waves and periodic waves under an ice sheet," *Philosophical Transactions of the Royal Society A: Mathematical, Physical & Engineering Sciences*, vol. 369, no. 1947, pp. 2957–2972, 2011.

[4] P. A. Milewski, J.-M. Vanden-Broeck, and Z. Wang, "Hydroelastic solitary waves in deep water," *Journal of Fluid Mechanics*, vol. 679, pp. 628–640, 2011.

[5] P. Wang and D. Lu, "Analytic approximation to nonlinear hydroelastic waves traveling in a thin elastic plate floating on a fluid," *Science China Physics, Mechanics & Astronomy*, vol. 56, no. 11, pp. 2170–2177, 2013.

[6] S. J. Liao, *Homotopy Analysis Method in Nonlinear Differential Equations*, Higher Education Press, Beijing, China, 2012.

[7] P. Wang and D. Q. Lu, "Nonlinear hydroelastic waves traveling in a thin elastic plate floating on a two-layer fluid," *Applied Mathematics and Computation*, vol. 274, pp. 700–710, 2016.

[8] R. M. S. M. Schulkes, R. J. Hosking, and A. D. Sneyd, "Waves due to a steadily moving source on a floating ice plate. Part 2," *Journal of Fluid Mechanics*, vol. 180, pp. 297–318, 1987.

[9] J. Bhattacharjee and T. Sahoo, "Interaction of current and flexural gravity waves," *Ocean Engineering*, vol. 34, no. 11-12, pp. 1505–1515, 2007.

[10] J. Bhattacharjee and T. Sahoo, "Flexural gravity wave generation by initial disturbances in the presence of current," *Journal of Marine Science and Technology*, vol. 13, no. 2, pp. 138–146, 2008.

[11] S. K. Mohanty, R. Mondal, and T. Sahoo, "Time dependent flexural gravity waves in the presence of current," *Journal of Fluids and Structures*, vol. 45, pp. 28–49, 2014.

[12] D. Q. Lu and R. W. Yeung, "Hydroelastic waves generated by point loads in a current," *International Journal of Offshore and Polar Engineering*, vol. 25, no. 1, pp. 8–12, 2015.

[13] S. J. Liao, *Beyond Perturbation: Introduction to the Homotopy Analysis Method*, CRC Press, Boca Raton, Fla, USA, 2004.

[14] Y. J. Jian, Q. Y. Zhu, J. Zhang, and Y. F. Wang, "Third order approximation to capillary gravity short crested waves with uniform currents," *Applied Mathematical Modelling*, vol. 33, no. 4, pp. 2035–2053, 2009.